© 1997 Oxford University Press
Nucleic Acids Research, 1997, Vol. 25, No. 15 **3095–3101**

Nanoscopic structure of DNA condensed for gene delivery

David D. Dunlap*, Alessia Maggi, Marco R. Soria and Lucia Monaco

DIBIT, San Raffaele Scientific Institute, via Olgettina 58, 20132 Milan, Italy

Received March 26, 1997; Revised and Accepted June 19, 1997

ABSTRACT

Scanning force microscopy was used to examine DNA condensates prepared with varying stoichiometries of lipospermine or polyethylenimine in physiological solution. For the first time, individual DNA strands were clearly visualized in incomplete condensates without drying. Using lipospermine at sub-saturating concentrations, discrete nuclei of condensation were observed often surrounded by folded loops of DNA. Similar packing of DNA loops occurred for polyethylenimine-induced condensation. Increasing the amount of the condensing agent led to the progressive coalescence or aggregation of initial condensation nuclei through folding rather than winding the DNA. At over-saturating charge ratios of the cationic lipid or polymer to DNA, condensates had sizes smaller than or equal to those measured previously in electron micrographs. Polyethylenimine condensates were more compact than lipospermine condensates and both produced more homogeneously compacted plasmids when used in a 2–4-fold charge excess. The size and morphology of the condensates may affect their efficiency in transfection.

INTRODUCTION

Unlike viruses, cationic molecules that bind to gene-carrying, plasmid DNA do not provoke immunological responses and pose no infection threat to patients. Their transfection efficiency may soon rival that of viral-mediated gene transfer *in vitro* and *in vivo* (1). The hypothesized mechanism of action is that, after charge neutralization and subsequent condensation of polyanionic DNA, the compacted plasmids are transported into cells by endocytosis and escape into the cytoplasm from endosomes (1–3). Subsequent transfer from the cytoplasm to the nucleus appears to be a critical barrier (1,2). A physical view of the condensates including their dimensions and DNA packing could facilitate improvement in the technology.

DNA condensation has been studied to understand charged polymer dynamics and also compaction into viral capsids, chromosomes and sperm heads (4). The formation of DNA condensates depends on soluble cations overcoming electrostatic repulsions. Indeed, Haynes *et al.* observed by electron microscopy that the forms of DNA condensed with poly-L-lysine depended on the ionic strength of the buffer (5). Their B-form DNA condensates included toroidal shapes that became the focus of further studies for the similarity to viral genomes (6). Chattoraj *et al.* reported nearly 80% toroidal shapes of condensates produced by excess spermidine in 2 mM NaCl (7). Similarly sized toroids resulted using DNA with a 4-fold difference in molecular weight. Even at ratios of 0.6 spermine/phosphate, toroids were detected if the DNA was sufficiently long to form a 70 nm diameter, circular template (8). Following these leads, Arscott and her collaborators experimentally measured average outer and inner diameters of hexamine cobalt-induced toroids, 90 and 35 nm respectively, and hypothesized that their size is governed by enthalpy where high order and 89% charge neutralization permit a packing density of 2.7 nm between DNA strands (9). They suggested that circumferential winding (10,11) of the DNA would require less energy and should be favored. Similarly sized, rod shaped condensates were noted, and different condensing agents produced different sizes of condensates and required different incubation times and concentrations (12). The authors proposed that sharp kinks may require longer time and stabilization to favor rod formation.

DNA condensates have also been studied for the purpose of developing protocols for gene therapy. Freeze–fracture electron micrographs of DNA mixed with cationic liposomes led to the proposal that intact liposomes bind DNA at low concentration, and fuse to encapsulate the DNA at higher concentrations (13). A separate study revealed that DNA mixed with DOTMA, a cationic lipid used for transfections, excluded ethidium bromide, a helix-intercalating fluorescent dye, at positive to negative charge ratios >1.1 (14). Electron microscopy of the condensates revealed increased compaction of the DNA as the ratio was increased from 0.2 to 1.5. The authors hypothesized that lipid vesicles bound to DNA at low concentration and, as the ratio of lipid to DNA was increased, DNA-catalyzed lipid fusion and cationic lipid-catalyzed DNA collapse cooperatively produced rod-shaped condensates. Very recent electron microscopy revealed lipospermine-induced condensates of ~100 nm diameter with tubular lipidic structure (2).

These reports identified conditions for DNA condensation with mechanistic insight in some cases. However, most condensates were formed in non-physiological solutions. Therefore this study was completed of DNA condensates prepared in physiological solution with a cationic lipid, lipospermine (dioctadecylamidoglycyl-spermine or DOGS) (15), and a cationic polymer,

*To whom correspondence should be addressed. Tel: +39 2 2643 4868; Fax: +39 2 2643 4813; Email: dunlapd@dibit.hsr.it

polyethylenimine (PEI) (16). These molecules have been used as DNA carriers for non-viral transfection of the rat kidney (17).

MATERIALS AND METHODS

Preparation of condensates

For all preparations, sterile distilled water (SALF, Bergamo, Italy) or MilliQ+ purified water (Millipore Inc., Bedford, MA, USA) was used. Other solutions used were 1 M HCl volumetric solution (J. T. Baker, Deventer, Holland), and 150 and 15 mM NaCl solutions prepared in the laboratory from dried salt (BDH Laboratory Supplies, UK). The NaCl solutions were filtered with Nalgene 0.2 μm syringe filters, and in some cases insoluble contaminants were removed by centrifugation. The DNA plasmids pSfiSVneo (7 kb), pSfiSVI9 (6 kb) and pCISfi-γIFN (5 kb) were propagated by standard techniques and purified on CsCl gradients (18). Stock solutions of the molecules used to condense DNA, 2 mM dioctadecylamidoglycylspermine (DOGS) in ethanol, and 10 mM polyethylenimine (PEI) 22 kDa (linear) or 25 kDa (25% N-branched) in water, were diluted in 150 mM NaCl or water for use. DNA condensates were prepared by mixing equal volumes of 40 ng/μl DNA solution and the indicated equivalents of condensing agent. Equivalents are defined as protonated nitrogen atoms for DOGS (three of the four nitrogen atoms at pH 7.4) and PEI (approximately one out of six of all nitrogen atoms at pH 7.4), and phosphate groups for DNA.

Scanning force microscopy

Condensates adhered to the imaging surface through electrostatic attraction. Substrates were freshly cleaved mica or mica coated with poly-L-ornithine (molecular weight 30 000–70 000; Sigma, St Louis, MO) by resting a 10 μl droplet of a 0.1 mg/ml poly-L-ornithine solution on the freshly cleaved mica for 1 min and rinsing with 11 drops of water or 150 mM NaCl.

Before imaging, all DNA condensate solutions were diluted 10–12.5 times to give DNA concentrations of ~2.4×10^{-6} M bp (~0.5–1 nM depending on plasmid length). For dry imaging, 5 μl of the diluted solution was spotted on the surface, rinsed with 11 drops of water after ~1 min, and then dried under a flow of nitrogen. For imaging in solution, the specimen was rinsed with 11 drops of the imaging solution, and covered with a few drops of the same fluid. To enhance adhesion of some condensates to the surface, the prepared substrate was submerged in 300 μl of the diluted condensate solution, and centrifuged for 10 min at 400 *g* and 21°C. The surface was then rinsed and imaged in solution.

Probe tips were chosen according to scanning conditions. Etched silicon tips, mounted on a single beam cantilever of length 125 μm and force constant in the range of 20–100 N/m, were used for dry imaging. For imaging in solution, oxide sharpened silicon nitride tips, mounted on a V-shaped cantilever, of length 120 μm and leg width of 40 μm were employed. The silicon nitride tips were agitated in a 2% solution of laboratory detergent for 15 min, rinsed in distilled water and then agitated overnight in a 1 M solution of HCl.

Images were recorded with a Nanoscope III Scanning Force Microscope (Digital Instruments, Inc., Santa Barbara, CA), operating in the tapping mode. The oscillation amplitude of the scanning tip registered 0.5 V and the frequency of the oscillation was in the range of 200–400 kHz dry or 10–40 kHz in solution. The scan rate was typically 1–2.5 Hz.

Images were processed and analyzed using the Nanoscope III software version 4.11 or Image SXM version 1.61, an extension of NIH Image for Macintosh computers (available from svr.ssci.liv.ac.uk/pub/Mac). Some images were 'flattened' by subtracting a first or second order polynomial from each scan line to remove offsets, tilts and bows. Particle areas were measured for those whose heights exceeded a user-defined threshold. Those <500 nm^2 (equivalent to a spherical diameter of 25.2 nm) were ignored, as they were unlikely to contain entire plasmids (see Discussion). Equivalent diameters for the particles were calculated assuming a circular geometry.

RESULTS

A scanning force microscope (19) was used to examine condensates. A typical scanning force micrograph is a color-encoded topograph formed by recording the separation necessary to

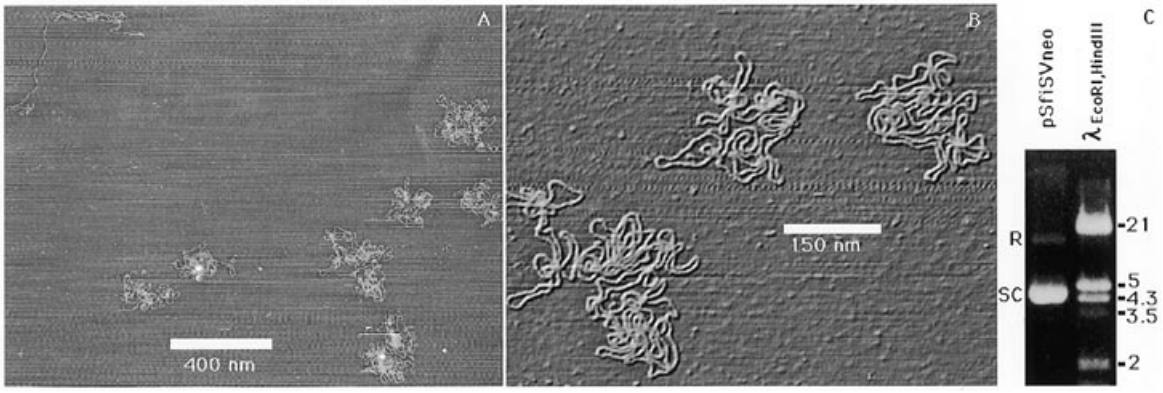

Figure 1. Scanning force micrographs of 7 kb plasmids in solution. Supercoiled plasmids were deposited on poly-L-ornithine-coated mica from a 150 mM NaCl solution and imaged in 15 mM NaCl. A low density of usually isolated plasmids was distributed on the surface (**A**). The color-encoded height scale extends 11.3 nm. Higher magnification with false illumination of the plasmids revealed many intersections between segments and long narrow loops (**B**) (image processing created the illuminated effect). One percent agarose gel electrophoresis of 500 ng of pSfiSVneo verified that most plasmids were supercoiled with only a minor proportion of nicked DNA (**C**). Bands corresponding to the relaxed (R) and supercoiled (SC) forms of pSfiSVneo are indicated beside fragments of λ DNA digested with the restriction enzymes *Eco*RI and *Hin*dIII.

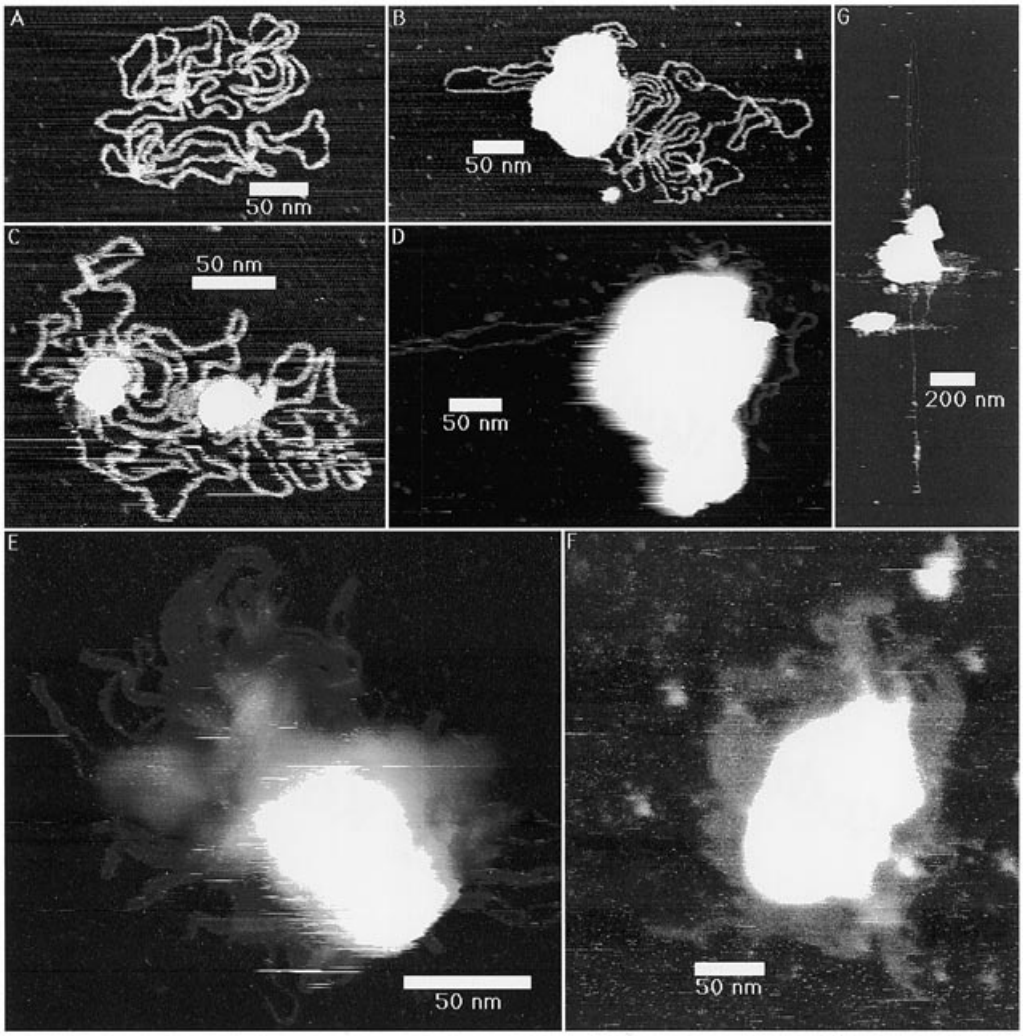

Figure 2. Diverse morphologies of unsaturated DOGS condensates. Condensates with 2 equivalents DOGS : 1 equivalent DNA were prepared and deposited on poly-L-ornithine-coated mica in 150 mM NaCl and topographically imaged in 15 mM NaCl. A mixture of forms was observed that ranged from uncondensed plasmids (**A**) to plasmids with discrete loci of condensation (**B** and **C**), to almost completely condensed plasmids (**D**). DNA was bundled in folded loops in the periphery of DOGS-condensates prepared identically and imaged in 15 mM NaCl (**E**) or 150 mM NaCl (**F**). Loops of DNA were extended by the scanning force microscope probe from a DOGS-condensate (**G**). Loops of DNA near the surface of the condensate were extended first vertically and then horizontally as the scan direction was rotated by 90°. The color-encoded height scale extends 5 nm (A–D and F), 25 nm (E) and 10 nm (G).

maintain a constant force between a spring-mounted stylus and a sample surface at each point in a scan. With a low contact force and a sharp stylus, the resulting image may reveal molecular topography.

This study included DOGS- and PEI-induced condensation of supercoiled plasmid DNA 5–7 kb in length. Electrostatically charged surfaces were used to attract and stabilize condensates from a droplet of solution. Unsaturated or incomplete condensates were presumed to have had negatively charged, peripheral loops of naked DNA which bound to positively charged, poly-L-ornithine-coated mica. Conversely, completely saturated condensates were supposed to have had only cationic lipid or polymer complexed DNA which therefore bound to negatively charged mica. By utilizing both substrates, oppositely charged species of heterogeneous populations of molecules were immobilized for examination by scanning force microscopy.

Plasmids deposited on poly-L-ornithine-coated mica

Figure 1 depicts typical plasmid molecules deposited on poly-L-ornithine-coated mica in 150 mM NaCl and imaged in a solution of 15 mM NaCl. The molecules were distributed at a low density on the surface which reflected the dilute nature of the deposition solution. Each plasmid had many intersections or cross-overs between segments which were often well separated along the contour of the plasmid and led to the formation of long narrow loops. Gel electrophoresis of the plasmid preparation (Fig. 1C) revealed that most plasmids were supercoiled, while only a small proportion was relaxed. No band corresponding to linearized DNA was visible. Seven kilobase pair plasmids prepared as described would be expected to have a superhelical density of –0.06 and thus one would expect 25–30 cross-overs in planar projections of them (20). In accordance with this expectation,

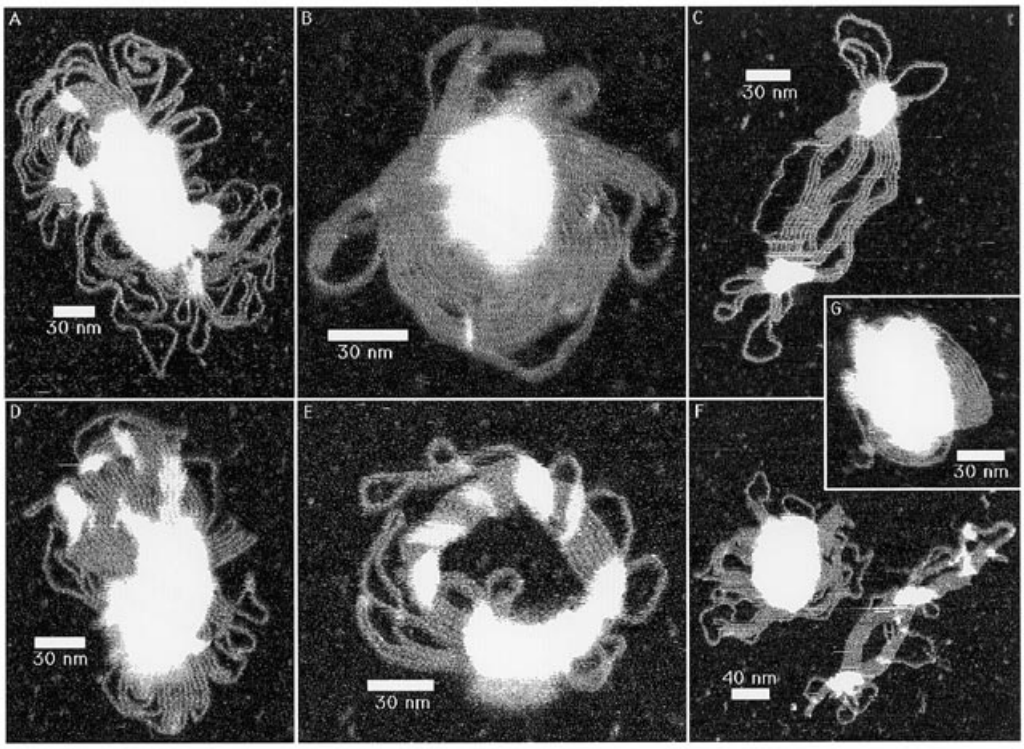

Figure 3. PEI condensates exhibit folded loops of DNA. PEI condensates prepared with 0.08 equivalents 22 kDa PEI : 1 equivalent DNA in 150 mM NaCl were deposited on poly-L-ornithine-coated mica and topographically imaged in 15 mM NaCl. Individual DNA strands can be traced and lateral packing of folded loops of DNA with sharp bends is common. DNA without PEI never assumed these forms. The color-encoded height scale extends 5 nm.

intersections counted in two tracings of a plasmid imaged at high resolution (Fig. 2A) numbered 20 or 28 depending on the paths chosen for strands passing through nodes.

Partial condensation with DOGS

DOGS, which is composed of a spermine head group with two hydrophobic tails, formed layers consistent with the dimensions of lipid bilayers when dried on mica from a concentrated ethanolic solution (data not shown). Depositing condensates prepared with 2 equivalents DOGS : 1 equivalent DNA on the positively charged, poly-L-ornithine-coated mica substrate produced a very heterogeneous preparation. On a single substrate visualized in 15 mM NaCl after deposition in 150 mM NaCl, a variety of condensed molecules was observed (Fig. 2A–D). Figure 2A depicts a plasmid with little or no DOGS while nearby plasmids had small (Fig. 2C) or large (Fig. 2B) globules attached or were almost completely condensed by the cationic lipid (Fig. 2D). This series of images prompted the speculation that condensation initiated at several sites and proceeded by aggregation or coalescence of these sites.

Particularly interesting are the radial loops in Figure 2 that may be an early step in condensation. While the peripheral DNA in most condensates had little order, the DNA of one condensate lay in bundles of folded loops with very sharp bends (Fig. 2E). Since high resolution imaging was more difficult at 150 mM NaCl, dependent on the characteristics of the probes, the concentration of NaCl was often decreased to 15 mM. Occasionally, a probe also functioned well enough to crudely visualize the structure of condensates in physiological solution. Figure 2F depicts such a condensate with a peripheral skirt of what was assumed to be DNA on the basis of its similarity to that observed clearly in lower ionic strength solution.

The partial DOGS condensates were characterized by loops of DNA radiating from one or more central cores. If this pattern of DNA folding were maintained in more complete condensates, the probe might have been able to hook and extend loops of DNA without displacing the condensate. In contrast easy extension of DNA loops would not have been possible in circumferentially wound structures. In Figure 2G, loops of DNA were fortuitously hooked and dragged by the probe as it scanned one condensate. Long loops of DNA were first extended above and below the core of the condensate while shorter loops were extended to the left and right after rotating the fast scan axis 90°.

In addition to the mixture of negatively charged, incomplete condensates, 2 equivalents DOGS : 1 equivalent DNA also produced compact, amorphous, positively charged condensates that bound to negatively charged mica (data not shown). The areas of such condensates were measured and corresponding diameters were calculated assuming circular shapes. A histogram of these data is shown in Figure 4 which the distribution ranged from 20 to 150 nm in diameter around a peak centered at 50–70 nm.

Partial condensation with 22 kDa PEI

For comparison, incomplete condensates were formed with a 0.08 : 1 equivalent ratio of linear, 22 kDa PEI : DNA. They were formed and deposited on poly-L-ornithine-coated mica in 150 mM

NaCl and subsequently imaged in 15 mM NaCl. Particularly high resolution images (Fig. 3), revealed a folded-loop structure very similar to that observed for DOGS-condensates. Individual strands of DNA were resolved separated and in bundles in which their spacing averaged 3.2 nm. Figure 3A and D depicts oblong condensates, but the folded-loops were more tightly packed in the condensate in Figure 3D. Very sharp bends can be traced in some of these loops. Figure 3C and F depict less compact, oblong condensates with multiple condensation nodes connected by bundles of DNA. One toroid was observed (Fig. 3E) and it seemed to result from circularization of a structure like that shown in Figure 3C. The joint seemed to be in the middle on the left side of the toroid which was partially obscured by PEI. Tight circular coils of DNA were also observed (Fig. 3B and G) Very sharp bends are visible in strands on the edge and in the interior of the condensate pictured in Figure 3B.

As with DOGS, PEI-induced condensation at less than saturating concentrations produced a heterogenous population of condensates. For example, 0.16 or 0.83 equivalents PEI : 1 equivalent DNA produced a mixture from which uncomplexed DNA, partially saturated condensates, and nearly saturated condensates adhered to poly-L-ornithine-coated mica while less compact PEI-coated plasmids bound to mica (Fig. 5). The less compact plasmids were assumed to have been covered with PEI in order to bind to mica, since DNA does not adhere to mica without positively charged ions. Thick segments represented either supercoils or bundles of these plasmids and the lower plasmid shown in Figure 5B seemed highly supercoiled. These images indicated that the polymer coated the entire length of the plasmid.

To further characterize the PEI condensates, the linear 22 kDa and branched 25 kDa PEI polymers were compared. The branched form appeared to be a more effective condensing agent, since linear 22 kDa but not branched 25 kDa PEI condensates bound to poly-L-ornithine-coated mica via naked DNA segments at a 0.08 : 1 equivalent ratio. Instead unsaturated condensates that adhered to poly-L-ornithine-coated mica were produced using 0.04 equivalents 25 kDa PEI : 1 equivalent DNA.

Complete condensation with DOGS

DNA plasmids became completely saturated in the range of 4–6 equivalents of DOGS : 1 of DNA. Attempts were made to image saturated condensates prepared in 150 mM NaCl and deposited on mica, but artifacts obscured dried preparations and imaging in solution was unstable probably because the probe quickly fouled. However at 4 : 1 equivalents, condensates prepared in water adhered to mica and produced a distribution of amorphous globules (data not shown) distributed similarly to the plasmids in Figure 1A. These condensates did not bind stably to poly-L-ornithine-coated mica which probably reflected their overall positive charge and the lack of naked DNA at the surface of the DOGS-saturated condensates. Their dimensions were similar to those produced with 2 equivalents DOGS : 1 equivalent DNA (Fig. 4).

Complete condensation with 22 kDa PEI

For comparison, PEI saturated condensates were prepared with 1.6 equivalents of 22 kDa PEI : 1 equivalent DNA which produced slightly positively charged condensates that were only detected after centrifugation of the condensates onto mica (data not shown). This presumably facilitated formation of a stable interaction with the surface. The vast majority of condensates

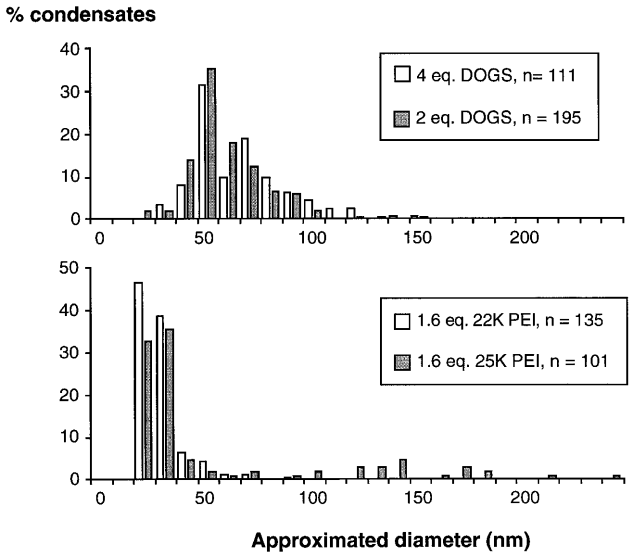

Figure 4. A histogram of condensate diameters. The areas of condensates were measured and diameters were calculated for equivalent circular areas. DOGS condensates were prepared using indicated equivalents : 1 equivalent DNA in water and dried for imaging. PEI condensates were prepared with 1.6 equivalents : 1 equivalent DNA in 150 mM NaCl and imaged in 15 mM NaCl. All condensates were deposited on mica.

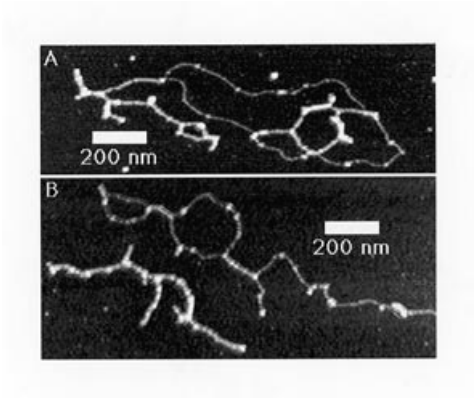

Figure 5. Plasmids coated with PEI. Condensates prepared with 0.16 equivalents 22 kDa PEI : 1 equivalent DNA in 150 mM NaCl were deposited on mica by centrifugation and dried for imaging. These PEI-coated plasmids found on the negatively charged mica may represent a more efficient transfectional form. The color-encoded height scale extends 3 nm.

were 20–40 nm in diameter for both the linear 22 kDa and branched 25 kDa PEI polymers, although a small number of much larger condensates resulted from condensation with branched 25 kDa PEI (Fig. 4). PEI condensates were smaller than those formed with DOGS.

DISCUSSION

Several factors determined what appeared in scanning force micrographs. First the condensates had to travel from within the droplet to the surface. Centrifugation enhanced this step for condensates with apparently low overall charge. Following that, the strength of the bond formed between the condensate and the surface determined whether subsequent rinsing to remove excess material also removed loosely-bound condensates. Centrifugation

may have also enhanced this step by holding condensates near the surface for long enough to establish stable interactions. The electrostatic charge of the surface determined what adhered and both negatively (freshly cleaved mica) and positively (poly-L-ornithine-coated mica) charged surfaces were employed to isolate condensates with opposite charges. Mica requires divalent cations or the poly-L-ornithine treatment in order to bind DNA, and therefore any condensates that attached securely to mica were assumed to be positively charged. Instead, the poly-L-ornithine-coated mica effectively bound naked DNA in solutions ranging from 0 to 150 mM NaCl.

Given that poly-L-ornithine-coated mica is such an avid substrate for DNA, it was particularly well suited for attracting condensates from the three-dimensional solute phase, and trapping them in two dimensions with the least possible distortion of their native structures. Such trapping ability was assessed through a test based on the fact that the average end-to-end distance of linear DNA molecules in three-dimensions is less than that of identical molecules constrained to two dimensions, and both may be calculated and compared to experimental values (21). In data not shown, the average end-to-end distance measured for linear DNA molecules of 2700 bp deposited on poly-L-ornithine was smaller than the calculated two-dimensional value. This indicated that the DNA molecules were quickly immobilized on the poly-L-ornithine surface in forms characterized by the smaller three-dimensional end-to-end distance and did not expand or equilibrate to their broader two-dimensional forms.

With this new method for isolating and examining individual condensates, ionic strength was found to strongly affect the resulting condensates as expected. Tangled, intermolecular condensation of plasmids occurred in condensation reactions containing 0.5 equivalents DOGS : 1 equivalent DNA in 150 mM NaCl while mostly isolated, partially condensed plasmids resulted from the same mixture made in water (data not shown).

It is noteworthy that the morphology of condensates was not limited to rods and toroids, probably because non-saturating ratios of DOGS and PEI were studied and the configurational variety shown in Figures 2 and 3 may have been better preserved in wet specimens. Complete condensates had rounded globular forms while unsaturated condensates ranged from bundled, folded loops of DNA surrounding central cores to loose coils with isolated nodes of condensation. Particularly interesting were the nodes of condensation induced by DOGS (Fig. 2B and C) that might represent intermediate steps in the transition from a random coil (Fig. 2A) to a condensed particle (Fig. 2D). Loops created by such nodes could easily adopt folded configurations. Progressive condensation from nodes was previously observed in electron micrographs of DNA condensed by cationic lipids (14). Lipid bilayer-covered DNA resulted, and including poly-L-lysine in the mixtures promoted 'spider-like' forms with central condensed cores and radiating loops. The morphologies observed here are consistent with those previous observations.

The similar structures observed in partial DOGS- and PEI-induced condensates are evidence of common mechanisms for DOGS- and PEI-mediated condensation of DNA. In Figure 2E, radial loops of DNA were observed in the periphery of a DOGS-condensate that were very similar to those observed in PEI-condensates (Fig. 3D). Such folded stretches of DNA have previously been inferred for condensed DNA in rod shapes (22) and most toroids which appear to result from the annularization of rods (9,23) (Fig. 3E). Acute bends were common in condensates contrary to previous speculation (12) and examinations of toroidal condensates in which circumferentially wound DNA was revealed (10,11). In the present experiments, such bends are likely the result of cationically catalyzed collapse of the loops of DNA characteristic of the supercoiled plasmids. Indeed, in Figure 1B, many loops with small radii of curvature are depicted. The cationic condensing agents merely had to reduce the electrostatic repulsion between looped DNA strands to fold them and create bundles.

Additionally, while thermodynamic constraints on such condensing DNA would favor mild distortions of the stiff polymer, kinetic limits may lead to other structures (4). An illustrative example of this kinetic folding problem is the coiling of rope. The torsional strain induced by coiling a short rope is readily relieved as the free ends twist. Instead torsional strain accumulates during coiling of a long rope where the free ends are tangled and heavy. This torsional strain interferes with coiling. Similarly, coiling a loop of rope without free ends produces torsional strain that cannot be relieved. An alternative to coiling rope is to fold it such that no torsional strain occurs. Then the strain occurs exactly at the bends in the rope.

Such folding is a consistent qualitative description for the molecules observed here and inhomogeneously distributes potential energy along DNA. Acute bends requiring much energy are compensated by adjacent bonding without the coordinated conformational changes along the entire length of a DNA molecule involved in coiling. Aggregation of DNA loops is typical of chromatin, which results in locally reversible and hierarchical condensation (24).

DNA strands folded and held with cationic glue contrasts with recent electron micrographs of tubular scaffolds of DOGS (2). These authors proposed that positively charged surfaces of closely packed, lipid tubules become wrapped in DNA. Their model is consistent with cooperative mechanisms of condensation in which DNA binds on the surface of positively charged lipidic structures at low equivalent ratios before becoming highly compacted at high ratios (13,14). In the present work no lipidic tubules were observed despite the fact that such tubules have been observed with scanning force microscopy (25). However, the linear 22 kDa PEI polymer used at 0.16 : 1 or 0.83 : 1 equivalents PEI : DNA did coat plasmids as shown in Figure 5. In these conditions, very few condensates or plasmids adhered to either the positively or negatively charged surfaces without centrifugation. With centrifugation, a dense clutter of slightly negatively charged debris accumulated on the positively charged surface while apparently polymer-coated DNA molecules adhered at a low surface density to an otherwise clean mica surface. Similarly condensed plasmids, that were formed in lower ionic strengths, have been observed previously by scanning force microscopy and suggested to be more efficient as transfection agents (26).

Another difference between DOGS- and PEI-mediated condensation was the size of complete condensates produced with DOGS or PEI. It is clear from Figure 4 that DOGS–DNA condensates averaged 50–70 nm in diameter and did not change appreciably between 2 and 4 equivalents DOGS : 1 equivalent DNA. Instead, PEI–DNA condensates produced with either linear 22 kDa or branched 25 kDa polymers were much smaller ranging from 20 to 40 nm in diameter. One reason is that the PEI condensates involved 5 kb plasmids while those in DOGS condensates were 6 kb. However, according to the following estimation other factors must have also been involved. The volume associated with

cylindrical approximations of B-form plasmids was assumed to equal the minimum volume of a spherical condensate. Then the diameter of spherical condensates calculated for the different plasmids were compared. One thousand additional base pairs in the DOGS condensates should have only increased the diameter of such a minimally sized condensate from 25.2 to 26.6 nm. The diameters found for PEI condensates lie in this range but DOGS condensates were much larger. Alternatively perhaps 2 or 4 equivalents of DOGS were insufficient to completely condense the plasmids. This is unlikely since 50–70 nm is less than the diameter previously established for toroidal condensates (9), 90 nm, DOGS condensates used in transfection experiments (2), 100 nm, and condensates formed with 12 equivalents poly-L-lysine : 1 equivalent DNA (27), 70–120 nm. A likely contribution to the increased compaction of PEI- versus DOGS-induced condensates is that the former were formed in 150 mM NaCl and the latter in water. Ionic strength has recently been shown to strongly affect the extent and form of DNA supercoiling which contributes to condensation (28). Ultimately, the polymer may be a more effective condensing agent than the lipid (12).

CONCLUSIONS

The similar structures observed for incomplete condensates formed with either DOGS or PEI suggest that a common condensation mechanism prevails in 150 mM NaCl. Plasmids condensed into bundled, folded loops of DNA likely reflect that most condensation proceeds through folding rather than winding DNA. Such folding is consistent with the hypothesis that circumferential or global winding of DNA strands like a ball of yarn is kinetically prohibited while cationically catalyzed, local folding of loops in supercoiled plasmids proceeds with rapid energy equilibration.

When condensates are used in transfection, excess amounts of cationic lipids or polycations are usually necessary to yield positively charged condensates (15,16). The present data indicate that such ratios produce more homogeneous, condensed plasmids the sizes of which are probably affected by the ionic strength of the solution. However the structural morphology may ultimately determine transfection efficiency (26), since DNA condensed with either cationic lipids (1) or polyamines (2) enters the cell without difficulty. In the present study, some PEI-condensed plasmids seemed to be coated by polymer rather than bundled in folded loops. Perhaps these forms constitute more effective transfection agents.

ACKNOWLEDGEMENTS

We gratefully acknowledge LOT Oriel Italia which provided the scanning force microscope, J. P. Behr who supplied DOGS and PEI reagents, anonymous referees for constructive criticism, and Alessandra Boletta for experimental assistance. The work was supported by grants to L. Monaco, Italian Telethon #D26, and to Flavia Valtorta, Italian Telethon #581, at the San Raffaele Scientific Institute. D.D. was a postdoctoral fellow of the Muscular Dystrophy Association and learned how to fold rope from Mark Leonard.

REFERENCES

1 Zabner, J., Fasbender, A. J., Moniger, T., Poellinger, K. A. and Welsh, M. J. (1995) *J. Biol. Chem.* **270**, 18997–19007.
2 Labat-Moleur, F., Steffan, A.-M., Brisson, C., Perron, H., Feugeas, O., Furstenberger, P., Oberling, F., Brambilla, E. and Behr, J.-P. (1996) *Gene Ther.* **3**, 1010–1017.
3 Zhou, X. and Huang, L. (1994) *Biochim. Biophys. Acta.* **1189**, 195–203.
4 Bloomfield, V. A. (1991) *Biopolymers* **31**, 1471–1481.
5 Haynes, M., Garrett, R. A. and Gratzer, W. B. (1970) *Biochemistry* **9**, 4410–4416.
6 Marx, K. A. and Ruben, G. C. (1983) *Nucleic Acids Res.* **11**, 1839–1854.
7 Chattoraj, D. K., Goshule, L. C. and Schellman, J. A. (1978) *J. Mol. Biol.* **121**, 327–337.
8 Marquet, R., Wyart, A. and Houssier, C. (1987) *Biochim. Biophys. Acta.* **909**, 165–172.
9 Arscott, P. G., Li, A.-Z. and Bloomfield, V. A. (1990) *Biopolymers* **30**, 619–630.
10 Marx, K. A. and Reynolds, T. C. (1982) *Proc. Natl. Acad. Sci. USA* **79**, 6484–6488.
11 Vengerov, Y. Y., Semenov, T. E., Streltsov, S. A., Makarov, V. L., Khorlin, A. A. and Gursky, G. V. (1985) *FEBS Lett.* **180**, 81–84.
12 Plum, G. E., Arscott, P. G. and Bloomfield, V. A. (1990) *Biopolymers* **30**, 631–643.
13 Sternberg, B., Sorgi, F. L. and Huang, L., (1994) *FEBS Lett.* **356**, 361–366.
14 Gershon, H., Ghirlando, R., Gutman, S. B. and Minsky, A. (1993) *Biochemistry* **32**, 7143–7151.
15 Behr, J.-P., Demeneix, B., Loeffler, J.-P. and Perez-Mutul, J. (1989) *Proc. Natl. Acad. Sci. USA* **86**, 6982–6986.
16 Boussif, O., Lezoualc'h, F., Zanta, M. A., Mergny, M. D., Scherman, D., Demeneix, B. and Behr, J. P. (1995) *Proc. Natl. Acad. Sci. USA* **92**, 7297–7301.
17 Boletta, A. *et al.* (1997) *Human Gene Ther.* in press.
18 Maniatis, T., Fritsch, E. F. and Sambrook, J. (1986) *Molecular Cloning: A Laboratory Manual*. Cold Spring Harbor Laboratory Press, Cold Spring Harbor, NY.
19 Hansma, P. K., Elings, V. B., Marti, O. and Bracker, C. E. (1988) *Science* **242**, 209–216.
20 Boles, T. C., White, J. A. and Cozzarelli, N. R. (1990) *J. Mol. Biol.* **213**, 931–951.
21 Bustamante, C. and Rivetti, C. (1996) *Annu. Rev. Biophys. Biomol. Struct.* **25**, 395–429.
22 Eickbush, T. H. and Moudrianakis, E. N. (1978) *Cell* **13**, 295–306.
23 Saenger, W. (1980) *Principles of Nucleic Acid Structure*. Springer-Verlag, New York.
24 van Holde, K. (1989) *Chromatin*. Springer-Verlag, New York.
25 Manne, S. and Gaub, H. E. (1995) *Science* **270**, 1480–1482.
26 Wheeler, C. J., Sukhu, L., Yang, G., Tsai, Y., Bustamante, C., Felgner, P., Norman, J. and Manthorpe, M. (1996) *Biochim. Biophys. Acta.* **1280**, 1–11.
27 Wolfert, M. A. and Seymour, L. W. (1996) *Gene Ther.* **3**, 269–273.
28 Lyubchenko, Y. A. and Shlyakhtenko, L. S. (1997) *Proc. Natl. Acad. Sci. USA* **94**, 496–501.